

Role of spin quantization in determining the thermodynamic properties of magnetic transition metals

F. Körmann,* A. Dick, T. Hickel, and J. Neugebauer

Max-Planck-Institut für Eisenforschung GmbH, D-40237 Düsseldorf, Germany

(Received 12 January 2011; revised manuscript received 22 February 2011; published 15 April 2011)

We propose a combined *ab initio*-spin quantum Monte Carlo (QMC) approach to compute thermodynamic properties of magnetic materials by first principles. The key to the proposed approach is a mapping of the magnetic long-range system onto an effective, nearest-neighbor quantum Heisenberg model, for which the QMC approach provides a numerically exact solution. The performance of the proposed method is demonstrated for the transition metals Fe, Co, and Ni by computing magnetization shapes, specific heat capacities, and free energies. Spin-quantization effects are found to be critical, even close to T_C .

DOI: [10.1103/PhysRevB.83.165114](https://doi.org/10.1103/PhysRevB.83.165114)

PACS number(s): 75.40.Cx, 71.15.-m, 75.50.Bb

I. INTRODUCTION

The rapid progress of first-principles methods, in particular density functional theory (DFT), allows nowadays an accurate parameter-free prediction of thermodynamic properties for a wide range of nonmagnetic materials.¹⁻³ A particular challenge is, however, the incorporation of magnetic excitations, which are mandatory for an accurate description of many of the technologically relevant structural and functional materials such as, e.g., steels,⁴⁻¹¹ magnetic shape memory alloys,¹² and half-metallic ferromagnets.¹³

A commonly employed approach to capture magnetic contributions is to combine DFT calculations with the Heisenberg model,^{11,14-20}

$$\mathcal{H}^{\text{mag}} = - \sum_{ij} J_{ij} \mathbf{S}_i \mathbf{S}_j, \quad (1)$$

where the $\mathbf{S}_{i,j}$ represent effective spin operators localized at lattice sites i, j , and the J_{ij} represents the exchange parameters. For the computation of the J_{ij} parameters within DFT, well-established approaches exist, such as the magnetic force theorem,²¹ or the frozen-magnon approach based on adiabatic spin dynamics.²²

To obtain finite-temperature properties, such as the Curie temperature T_C , the magnetic contribution to the specific heat capacity $C_p(T)$, or free energy $F(T)$, a numerically accurate solution of the quantum model (1) is critical. In principle, a straightforward method is given by the spin quantum Monte Carlo (QMC) method. In practice, however, this method is severely limited by the negative-sign problem, which occurs if any form of magnetic frustration is present. This problem arises due to the fact that the quantum-mechanical expectation value is mapped onto a classical one: The resulting weights (probabilities) may become negative, making the QMC approach impractical.²³ The sign problem is a serious and often prohibitive obstacle in applying the QMC method for realistic systems, where the J_{ij} parameters are typically long range and show a Ruderman-Kittel-Kasuya-Yosida (RKKY)-type oscillating (ferromagnetic, antiferromagnetic) behavior.

Due to the sign problem, one is typically forced to solve the Heisenberg Hamiltonian approximately. Common approximations are the analytic random-phase approximation (RPA) or classical Monte Carlo (CMC) calculations. Both

yield reliable predictions of selected data, such as the Curie temperature T_C .^{11,15-20} Recent studies, however, show that severe limitations arise^{11,20} when applying these concepts to access temperature-dependent properties such as, e.g., heat capacities: While the analytic RPA is found to provide excellent agreement with available experimental data up to T_C , it does not capture local magnetic order above T_C , giving rise to clear deviations in this temperature range.¹¹ In contrast, CMC works well at higher temperatures (above T_C), but fails at lower temperatures due to the neglect of spin quantization.²⁰ Also, both approaches show clear deficiencies in predicting net magnetization curves $M(T)$.¹¹

An important step toward making the available spin QMC methods applicable to realistic long-range and weakly frustrated magnetic systems (and thus including spin-quantization in realistic materials) would be a prescription that allows one to map the full Hamiltonian [Eq. (1)] onto a frustration-free and, ideally, short-range effective magnetic system without losing relevant information. Recent studies showed that while the type of magnetism (ferromagnetic, antiferromagnetic) or the inclusion of second or more interaction shells may have a significant impact on T_C , the rescaled shape of thermodynamic quantities, such as the heat capacity $C_p(T/T_C)$, is largely independent.²⁰ This remarkable insensitivity indicates that the full long-range spin Hamiltonian may be transformed into a nearest-neighbor model with effective exchange interactions. As will be demonstrated, this transformation gives an excellent approximation to the full Hamiltonian (provided that the T_C of the full model is reproduced) and can be readily solved by standard QMC calculations.

Furthermore, as will be shown in the following, this approach works remarkably well and provides an accurate description of the thermodynamic properties for often-studied magnetic benchmark systems (Fe, Co, and Ni). The proposed approach also dramatically improves the description of the net magnetization compared to existing *ab initio* approaches, and has similar accuracy to empirically fitted approaches,³⁰ yet is fully *ab initio*.

II. THEORY

To allow a direct comparison with experimentally accessible quantities, we compute in the following the full free energy.

Following our previous studies,^{11,20} we decompose the free energy $F(T, V)$ into electronic, vibronic, and magnetic contributions. The specific heat capacity at constant pressure is obtained via $C_P(T) = -T(\frac{\partial^2 F(T, V)}{\partial T^2})_{V, P}$. Electronic and vibronic contributions have been evaluated using the quasiharmonic approximation and finite-temperature DFT, respectively, as in Refs. 11,20,31. The DFT calculations are performed with the VASP³² package using the projector augmented-wave (PAW) method³³ within the generalized gradient approximation (Perdew-Burke-Ernzerhof parametrization).³⁴ The numerical parameters have been carefully chosen to ensure a numerical convergence of < 1 meV per atom in the considered temperature range.³⁵ The QMC calculations are done employing the direct-loop algorithm in the stochastic series expansion, as implemented in the ALPS code.³⁶ Monte Carlo calculations involve 2.5×10^6 steps, including thermalization and statistical averaging. The model calculations are carried out for three different system sizes ($N = 512, 1728, \text{ and } 5832$) to estimate the impact of finite-size effects.

To construct an effective spin Hamiltonian that can be solved by the QMC method, three ingredients are needed: (i) the crystallographic structure of the spin lattice, (ii) the spin quantum number S , and (iii) the effective interaction parameter J_{eff} . The first ingredient, the crystallographic structure, is given by the position of all atoms exhibiting local magnetic moments. For the unary transition metals considered here, these are simply the bcc and fcc lattice sites. For alloys consisting of magnetic and nonmagnetic or weakly magnetic atoms, only the positions of the magnetic ones are used. The second ingredient, the spin quantum numbers \bar{S} , are defined via the theoretical ground-state magnetic moments M_0 ,³⁷ as $\bar{S} = M_0/(g\mu_B)$, where $g \approx 2$ denotes the Landé factor.

The third ingredient, the effective interaction parameter J_{eff} , has to be constructed such that the corresponding effective Hamiltonian reproduces the correct T_C . The change of the effective parameters due to thermal volume expansion is expected to be a small effect, and is neglected in this study. The remaining task is the determination of T_C . In principle, T_C can be determined fully *ab initio*, e.g., by calculation of all J_{ij} parameters and using approximate methods such as RPA,^{11,17,18} renormalized RPA,³⁸ CMC,^{6,15,16,20} or extended Heisenberg models.^{6,39} In order to avoid additional approximations, we use in the present study the experimental value⁴⁰ to assign the resulting errors solely to the mapping onto the effective Hamiltonian. We note that the proposed mapping procedure is based on the empirical observation that spin systems with very different spin interaction parameters give almost identical $C_P(T)$ curves, provided that the resulting critical magnetic temperature is identical. A mathematical formulation expressing this relation and showing the underlying approximations would be desirable but is yet lacking. Following the above steps, the effective Hamiltonian is constructed and solved using the QMC method. Based on these calculations, the heat capacity is obtained by employing the fluctuation-dissipation theorem. The magnetic contribution to $F(T, V)$ is computed combining the magnetic inner energy $U = \langle \mathcal{H} \rangle$ (which is directly obtained in the QMC calculations), with the magnetic entropy determined by integrating the heat capacity.

III. RESULTS

To check the reliability and accuracy of the effective Hamiltonian, we first investigated and analyzed the temperature dependence of the net (reduced) magnetization $M(T)/M_0$. As has been shown in previous studies, even sophisticated approaches fail to give an accurate description of the magnetization shape. For example, for bcc Fe, the RPA gives a very good qualitative description of T_C , C_P , and F when using DFT-computed spin-interaction parameters, but fails to accurately describe $M(T)/M_0$.¹¹ Similar observations have been made for classical Monte Carlo approaches.²⁰ As a consequence, the magnetization shape is commonly not described using *ab initio*-derived spin-interaction parameters. Rather, approximate physical models with parameters fitted to experimental data are used.³⁰ This empirical model showed a universal relationship and has been successfully applied to a wide range of magnetic materials.

The magnetization shape, as obtained from the effective Hamiltonian using the QMC method, is shown in Fig. 1 (first column). The magnetization shape shows significant finite-size effects. To analyze these effects in more detail, we show results for three different system sizes ($N = 512, 1728, \text{ and } 5832$). As can be seen, the largest cell provides converged results (with respect to the cell size) for reduced temperatures below $T/T_C \approx 0.95$. Above this value, finite-size effects can no longer be neglected. Fig. 1 shows that below this value an excellent agreement with the experimental data is achieved. The agreement of the QMC-computed magnetization shape (i.e., fully *ab initio*) is comparable to the established Kuz'min's empirical approach.³⁰

The fact that classical Monte Carlo method fails to accurately describe the magnetization shape indicates that finite-temperature magnetization is substantially affected by spin-quantization effects. By performing classical Monte Carlo calculations using a nearest-neighbor Hamiltonian, which reproduces the same T_C , we have a unique opportunity to quantify the quantum effects. As can be seen in Fig. 1, the magnetic contributions (shaded magenta regions) are substantial, even at high temperatures (i.e., close to T_C), where quantum effects are often assumed to be negligible. They are also responsible for ensuring the exact Bloch $T^{3/2}$ relation for low temperatures and are clearly significant in obtaining the overall agreement. The good agreement between the classical and the quantum-mechanical calculation around and above T_C indicates that better converged results in this region can be achieved by classical calculations that are numerically much less expensive.

Having verified the performance of the effective Hamiltonian, we consider now the specific heat capacity C_P . Its computed temperature dependence is shown in Fig. 1 (second column) together with experimental data obtained at zero pressure.⁴¹ To better understand the role of the magnetic contributions, we first consider vibronic and electronic contributions only. As can be seen in Fig. 1 (second column), up to a temperature of ≈ 300 K, the agreement is excellent: The magnetic contribution in this range is negligible, indicating that the studied systems are still strongly magnetically ordered up to this temperature. Going above room temperature, the magnetic contribution becomes clearly relevant for all three

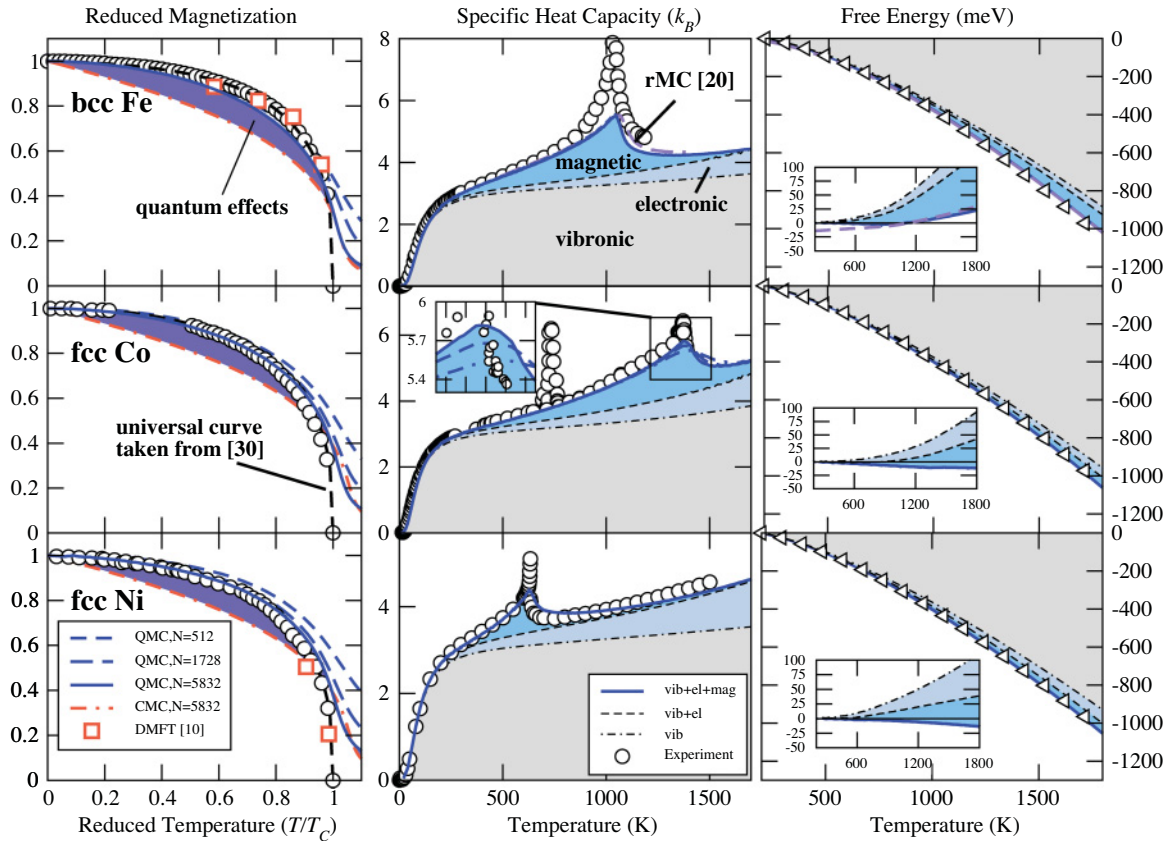


FIG. 1. (Color online) Reduced magnetization $M(t)/M_0$ (first column), specific heat capacity $C_p(T)$ (second column), and free energy $F(T)$ (third column) are shown for Fe, Co, and Ni in comparison with experimental results (Refs. [24–28]) and data obtained by the CALPHAD approach, employing the THERMOCALC program and the SGTE unary database (Ref. [29]). For Fe (first row), the results of [20] are shown for comparison.

materials. Analyzing the various free-energy contributions, it becomes obvious that the electronic contribution increases from Fe over Co and is highest for Ni. This is inherently connected with the magnitude of the band splitting being smallest in the case of Ni (of the order of the thermal energy $\sim 0.2\text{--}0.3$ eV). Due to the small splitting, both the spin-up and spin-down channel are only partially occupied, thus giving rise to a substantial electronic entropy.

Adding the magnetic contribution significantly affects the heat capacity over a large temperature window around T_C . As can be seen in Fig. 1 (second column), the magnetic contribution is smallest for Ni. This is a direct consequence of the fact that the spin quantum number \bar{S} is smallest for this element. The figure also shows that for all three studied metals, the agreement of the resulting total heat capacity with the experimental data is excellent. The largest discrepancies are found close to T_C , particularly for Fe. This may be related to finite-size effects in the QMC calculations, which are particularly relevant near the critical point. Also, experimental scatter is largest around T_C due to the rapid change in C_p around the critical point.^{24–28}

To further analyze the performance of the effective Hamiltonian, we consider the Helmholtz free energy. The results are shown in Fig. 1 (third column). Also shown are free energies derived from experimental calorimetric data within a CALPHAD approach. In order to allow a direct comparison

between the *ab initio* results and the results obtained by the CALPHAD approach, we follow previous studies^{3,11,20} and align both data sets at 200 K. Similarly as for C_p , we first consider the vibronic and electronic contributions. As can be seen in Fig. 1 (third column), the agreement up to room temperature is excellent. Errors are < 2 meV. A closer inspection shows that the electronic contribution to the free energy increases from Fe over Co, and reaches its maximum for Ni (≈ 70 meV at $T = 1800$ K). The origin is similar as for C_p , and is the decrease in band splitting from Fe towards Ni.

The addition of the magnetic contribution results in an excellent agreement with the experimental data for all three metals. The magnitude of the magnetic contribution shows a reversed trend as observed for the electronic contribution: The strongest magnetic contribution is obtained in case of bcc Fe (≈ 100 meV at the highest temperature $T = 1800$ K considered here). The reason is that among the studied elements, Fe has the highest spin quantum number ($\bar{S} \approx 1.1$). Interestingly, although Co has a larger spin quantum number than Ni, their magnetic contributions are comparable. The reason for this deviation from the general trends is the low T_C of Ni. Due to this already occurring at moderate temperatures, the spin system is close to the fully disordered state, whereas in the same temperature window, a noticeable amount of magnetic energy in Co is still stored in the magnetic short-range order. Comparing the free energies (including all contributions) with

the CALPHAD values, we observe an excellent agreement for all three studied metals. The strongest deviations are observed for bcc Fe (≈ 30 meV at $T = 1800$ K) due to the poor description of C_P around T_C (see Fig. 1, second column), whereas a nearly perfect quantitative agreement is obtained for Co and Ni (≈ 10 meV at $T = 1800$ K).

IV. CONCLUSION

In conclusion, we propose a straightforward mapping procedure that transforms the full magnetic Hamilton operator of realistic systems with long-range and oscillating interactions onto an effective Hamiltonian with nearest-neighbor effective interactions only. The effective interaction parameter is constructed such that the effective model reproduces the T_C of the full magnetic Hamiltonian. The approach allows one to decouple the estimation of T_C —for which it is well known that for some materials (e.g., Ni) mechanisms such as longitudinal spin fluctuations are critical—from the determination of other thermodynamic properties. In contrast to the full Hamiltonian, the effective model is free of any frustrations in the spins and can be thus efficiently solved by the spin QMC method. Combining the QMC results with vibronic and electronic free-energy contributions allowed us to carefully

and systematically compare the performance and accuracy of this approach with available experimental data. Generally, an excellent agreement has been found with small restrictions to the region closely around T_C , where finite-size effects become substantial. The strong impact of spin quantization on thermodynamic properties even at temperatures close to T_C is remarkable, and highlights the importance of developing approaches that are able to take these effects accurately into account.

ACKNOWLEDGMENTS

Discussions with Blazej Grabowski and Andrew Duff are gratefully acknowledged. Funding by the collaborative research center, SFB 761 “Stahl-*ab initio*,” of the Deutsche Forschungsgemeinschaft and the Interdisciplinary Centre for Materials Simulation (ICAMS), which is supported by ThyssenKrupp AG, Bayer MaterialScience AG, Salzgitter Mannesmann Forschung GmbH, Robert Bosch GmbH, Benteler Stahl/Rohr GmbH, Bayer Technology Services GmbH and the state of North-Rhine Westphalia, as well as the European Commission in the framework of the European Regional Development Fund (ERDF) is gratefully acknowledged.

*koermann@mpie.de

¹P. Souvatzis and O. Eriksson, *Phys. Rev. B* **77**, 024110 (2008).

²A. Siegel, K. Parlinski, and U. D. Wdowik, *Phys. Rev. B* **74**, 104116 (2006).

³B. Grabowski, T. Hickel, and J. Neugebauer, *Phys. Rev. B* **76**, 024309 (2007).

⁴B. Hallstedt, D. Djurovic, J. von Appen, R. Dronskowski, A. Dick, F. Körmann, T. Hickel, and J. Neugebauer, *Calphad* **34**, 129 (2010).

⁵S.-L. Shang, Y. Wang, and Z.-K. Liu, *Phys. Rev. B* **82**, 014425 (2010).

⁶M. Y. Lavrentiev, D. Nguyen-Manh, and S. L. Dudarev, *Phys. Rev. B* **81**, 184202 (2010).

⁷C. M. Fang, M. H. F. Sluiter, M. A. van Huis, C. K. Ande, and H. W. Zandbergen, *Phys. Rev. Lett.* **105**, 055503 (2010).

⁸H. Hasegawa and D. G. Pettifor, *Phys. Rev. Lett.* **50**, 130 (1983).

⁹L. Sandoval, H. M. Urbassek, and P. Entel, *Phys. Rev. B* **80**, 214108 (2009).

¹⁰A. I. Lichtenstein, M. I. Katsnelson, and G. Kotliar, *Phys. Rev. Lett.* **87**, 067205 (2001).

¹¹F. Körmann, A. Dick, B. Grabowski, B. Hallstedt, T. Hickel, and J. Neugebauer, *Phys. Rev. B* **78**, 033102 (2008).

¹²M. A. Uijtewaal, T. Hickel, J. Neugebauer, M. E. Gruner, and P. Entel, *Phys. Rev. Lett.* **102**, 035702 (2009).

¹³M. Lezaic, P. Mavropoulos, J. Enkovaara, G. Bihlmayer, and S. Blügel, *Phys. Rev. Lett.* **97**, 026404 (2006).

¹⁴S. V. Halilov, A. Y. Perlov, P. M. Oppeneer, and H. Eschrig, *Europhys. Lett.* **39**, 91 (1997).

¹⁵M. Ležaić, P. Mavropoulos, and S. Blügel, *Appl. Phys. Lett.* **90**, 082504 (2007).

¹⁶A. V. Ruban, S. Khmelevskiy, P. Mohn, and B. Johansson, *Phys. Rev. B* **75**, 054402 (2007).

¹⁷M. Pajda, J. Kudrnovsky, I. Turek, V. Drchal, and P. Bruno, *Phys. Rev. B* **64**, 174402 (2001).

¹⁸F. Körmann, A. Dick, T. Hickel, and J. Neugebauer, *Phys. Rev. B* **79**, 184406 (2009).

¹⁹L. Bergqvist, B. Belhadji, S. Picozzi, and P. H. Dederichs, *Phys. Rev. B* **77**, 014418 (2008).

²⁰F. Körmann, A. Dick, T. Hickel, and J. Neugebauer, *Phys. Rev. B* **81**, 134425 (2010).

²¹A. Liechtenstein, M. Katsnelson, and V. A. Gubanov, *J. Phys. F* **14**, L125 (1984).

²²See, e.g., Ref. 14. We note that within the adiabatic treatment, the fast, single spin-flip degrees of freedom of individual electrons (Stoner excitations) are integrated out. Alternatively, magnetic excitation can be determined via the transversal spin susceptibility, but requires the time-dependent formulation of DFT (see, e.g., Ref. 42) or many-body perturbation theory (see, e.g., Ref. 43).

²³E. Y. Loh, J. E. Gubernatis, R. T. Scalettar, S. R. White, D. J. Scalapino, and R. L. Sugar, *Phys. Rev. B* **41**, 9301 (1990).

²⁴*Magnetic properties of Metals*, edited by H.P.J. Wijn, K.-H. Hellwege, and O. Madelung, Landolt-Börnstein, New Series, Group III, Vol. 19a, p. 37 (Springer-Verlag, Berlin, 1981).

²⁵P. D. Desai, *J. Phys. Chem. Ref. Data* **15**, 967 (1986).

²⁶Q. Chen and B. Sundman, *J. Phase Equilib.* **22**, 631 (2001).

²⁷Y. S. Touloukian, R. K. Kirby, R. E. Taylor, and P. D. Desai, *Thermophysical Properties of Matter* (Plenum, New York, 1975), Vol. 12.

²⁸A. F. Guillermet, *Int. J. Thermophys.* **8**, 481 (1987).

²⁹A. F. Guillermet and P. Gustafson, *High Temp.-High Press.* **16**, 591 (1985).

³⁰M. D. Kuz'min, *Phys. Rev. Lett.* **94**, 107204 (2005).

³¹X. Sha and R. E. Cohen, *Phys. Rev. B* **73**, 104303 (2006).

- ³²G. Kresse and J. Furthmüller, *Phys. Rev. B* **54**, 11169 (1996).
- ³³P. E. Blöchl, *Phys. Rev. B* **50**, 17953 (1994).
- ³⁴J. P. Perdew, K. Burke, and M. Ernzerhof, *Phys. Rev. Lett.* **77**, 3865 (1996).
- ³⁵Vibrational part: 54/108 atom supercell (bcc/fcc); 27 000 \mathbf{k} -points per atom (kp-a); plane-wave cutoff energy $E_{\text{cut}} = 340$ eV. Electronic part: 40 000 kp-a; $E_{\text{cut}} = 340$ eV.
- ³⁶A. Albuquerque, F. Alet, P. Corboz, P. Dayal, A. Feiguin, S. Fuchs, L. Gamper, E. Gull, S. Gürtler, A. Honecker, R. Igarashi, M. Körner, A. Kozhevnikov, A. Läuchli, S. Manmana, M. Matsumoto, I. McCulloch, F. Michel, R. Noack, G. Pawłowski, L. Pollet, T. Pruschke, U. Schollwöck, S. Todo, S. Trebst, M. Troyer, P. Werner, and S. Wessel, *J. Magn. Magn. Mater.* **310**, 1187 (2007).
- ³⁷In itinerant systems, \bar{S} can be any number, $\bar{S} \in \mathfrak{R}$. For quantities $\bar{f}(T, \bar{S})$, exact solutions for $S_1 \leq \bar{S} \leq S_2$ ($S_2 - S_1 = 1/2$) are computed and a linear interpolation is employed afterwards, i.e., $\bar{f}(T, \bar{S}) = \alpha f(T, S_2) + (1 - \alpha) f(T, S_1)$, with $\alpha = 2(\bar{S} - S_1)$. The computed ground-state moments for Fe, Co, and Ni are 2.21, 1.64, and $0.63\mu_B$. For the latter, an extrapolation is used to compute $\bar{S} = 0.3$.
- ³⁸P. Bruno, *Phys. Rev. Lett.* **90**, 087205 (2003).
- ³⁹S. Shallcross, A. E. Kissavos, V. Meded, and A. V. Ruban, *Phys. Rev. B* **72**, 104437 (2005).
- ⁴⁰The experimental T_C^{exp} are 1044 K (Fe), 1388 K (Co), and 631 K (Ni).
- ⁴¹The first peak in Co at ≈ 700 K occurs due to a structural hcp-fcc transition. This transition is *not* included in our study, where the focus is on magnetic transitions. Since the magnetic transition occurs in the fcc phase of Co, we consider only this structure here.
- ⁴²S. Y. Savrasov, *Phys. Rev. Lett.* **81**, 2570 (1998).
- ⁴³E. Sasioglu, A. Schindlmayr, C. Friedrich, F. Freimuth, and S. Blügel, *Phys. Rev. B* **81**, 054434 (2010).